Journal of Multidisciplinary Sciences
www.multidisciplines.com

Estimate the depth to basement from the interpretation of aeromagnetic data at the northwestern part of Egypt

Gamal Zidan Abdelaal[1*], Mohamed Kamel Mohamed Mousa[2], and Mohamed Osman Ebraheem[2]
[1]*Geology Department, Faculty of Science, Assiut University, Assiut, 71516, Egypt.*
[2]*Geology Department, Faculty of Science, New Valley University, El Kharga, 72511, Egypt.*
[*]*Corresponding author email address: zidan@aun.edu.eg*

Received: 18 March 2021; Accepted: 14 May 2021; Published online: 20 May 2021

Abstract. The northwestern Sahara represents one of Egypt's most important oil and gas production and agricultural projects. This paper deals with the interpretation of aeromagnetic data to map the basement depth at the northwestern part of Egypt. The aeromagnetic data of the study area presented as International Geodetic Reference Formula (IGRF) map and has been digitized and processed using the Geosoft Oasis Montaj software. The local and deep magnetic sources were separated using Butterworth filters. The basement was estimated using the radial average power spectrum technique (RAPS), the source imaging parameter method, and the Euler Deconvolution technique. The RAPS technique revealed that the average depth to shallow and deep magnetic sources (basement) is about 1540 m and 6960 m, respectively, while the SPI technique showed that the basement depth ranged from 2529 m to 5559 m over the study site. The obtained ED anomalies range from 1065 to 4526 m in depth. It is noted that the depth increases northward the study area. Results denote that northern and southeastern parts distinguish deeper basement sources; the depth reaches 5559 m. These parts have a thick sedimentary cover due to the subsidence of these parts representing the basins that have the potentiality for hydrocarbon and underground water exploration.

Keywords: aeromagnetic, depth to basement, Euler Deconvolution, radial average power spectrum, source parameter imaging, Hydrocarbon, and groundwater potentiality.

Cite this as: Abdelaal, G.Z., Mousa, M.K.M. & Ebraheem, M.O. (2021). Estimate the depth to basement from the interpretation of aeromagnetic data at the northwestern part of Egypt. J. Multidiscip. Sci. 3(1), 27-38.

1. Introduction

Aeromagnetic survey one of the most effective tools in the investigation of sedimentary basins, in terms of potential hydrocarbons and underground water, which provide information about basement rocks depth and geological structures that have affected overlying Sedimentary rocks (Donaldson et al.,1998; Ross and Eaton, 1999; Kumar et al., 2006; Abu El Ata et al., 2013; Haby et al., 2016; Khalil et al., 2016; Hesham et al., 2016). The primary purpose of an aeromagnetic survey is to investigate subsurface geological setting based on differences in the magnetic field of the earth, which appear as anomalies resulting from magnetic susceptibility contrast between the basement and sedimentary rocks, magnetic properties of sedimentary rocks are less than the basement rocks (Reynolds, 1997).

The area under investigation is located in the northwestern desert of Egypt at the intersection of longitude and latitude, E 24°30 to 29° E and N 29° to 31°45' respectively (Figure 1). North Western Desert has stratigraphic succession from Paleozoic to Cenozoic era, distributed in four basins: Abu Gharadig, Alamein, Matruh-Shoshan, and Fagur (Shahin, 1989). It is one of the most important oil and gas production and agricultural projects in Egypt, many studies carried out for this purpose;(Bayoumi et al., 1989; Nessim et al., 1992; Bayoumi, 1996; Metwaly et al., 2009; Elkhodary et al., 2013; Yousef et al., 2016; Adel et al., 2016; Naser et al., 2017; Ismail et al., 2017; Rabeh et al., 2017).

The main purpose of interpretation of the aeromagnetic data is estimating and mapping of the basement depth and consequently determination of sedimentary cover thickness to determine locations of sedimentary basins in which it is possible to have hydrocarbon or groundwater based on the International geodetic reference formula (IGRF) and Butterworth technique in the low pass and high pass separation. In addition to quantitative interpretation used Radial Average Power Spectrum (RAPS), Source Parameter Imaging (SPI), and Euler Deconvolution as depth estimation techniques which, were processed with Geosoft oasis montaj v.8.4 (2015). The geophysical and geological data used for this purpose are: reduced to pole map of the study area (scale 1: 500,000) prepared by "western atlas international" for EGPC (1989), the geological map of Egypt (scale 1:500.000) published by EGPC and Conoco (1987) and accurate depths of drilled wells from public data.

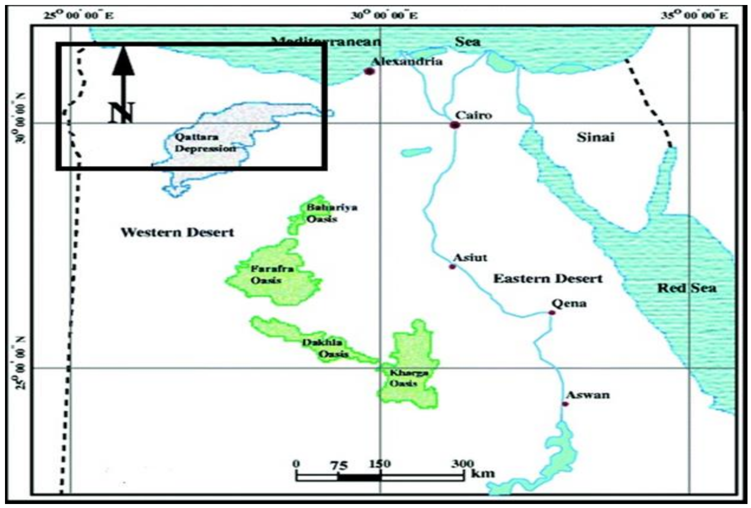

Figure 1. Location map of the study area.

2. Materials and methods

2.1. Experiment conducted area

The Western Atlas International established the Aeromagnetic data for EGPC (1989) for oil and gas exploration. The geological map of Egypt (scale 1:500.000) published by EGPC and Conoco (1987) and accurate depths of drilled wells from public data.

The aeromagnetic map was digitized using Geosoft Oasis montaj software version 8.4 (2015). Aeromagnetic data is being filtered using Butterworth filter operators to improve the signal properties of the available data (Hesham et al., 2016). The IGRF technique is used to remove the regional effects of the earth's magnetic field. Butterworth low pass and high pass filters applied with parameters of, degree of filter function are 8; the central wave numbers are 0.043 and 0.48 (cycle/ground unit), respectively and 0/1 A flag. Butterworth high-pass filters are used to focus on detail on maps, with taking a risk to improve noise (Cooper, 1997). Butterworth low pass filter is used to remove local variations and noise to improve regional magnetic anomalies. Application of the radial average power spectrum (RAPS) technique, the source parameter imaging technique (SPI), and Euler deconvolution was very effective in estimating the depth of the basement using the Geosoft Oasis montaj software version 8.4 (2015).

Spectrum analysis technique applied to estimate the depth of magnetic anomalies has been discussed by many authors (Bhattacharyya, 1966, 1978; Cassano and Rocca, 1975; Gerard and Debeglia, 1975; Hahn et al., 1976; Fedi et al., 1997; Saibi et al., 2016; Subrahmanyam and Gebissa, 2017). The radial average power spectrum technique was set for quantitative studies of magnetic anomalies. The logarithm of RAPS (square of Fourier amplitude spectrum) versus radial frequency. The slopes of the linear portions of the spectrum correspond to separate depth groups and provide the parameters used to design many of the enormous filters (Kivior and Byod, 1998; Spector and Grant, 1970) developed a depth profiling method to calculate the power spectrum of magnetic grids for depth estimation by the formula:

$$h \text{ (depth)} = -\text{slope}/4\pi \ldots\ldots\ldots\ldots\ldots (1)$$

The source parameter imaging method is a rapid and easy method for depth estimation of magnetic sources. The accuracy of SPI is like the Euler deconvolution method. Although, the SPI technique produces a full range of points of solution clear and easy to use. (Thurston and Smith, 1997) indicate that the results of SPI are easily interpreted. The main advantages of the SPI method over other techniques are the absence of a Data window moving, the calculation does not take a long time, and noise errors can be reduced by carefully sorting the data before calculating the depth. Euler deconvolution technique based on the

Euler's equation as developed (Reid et al., 1990) and have explained the methodology in detail for depth estimation of magnetic sources (Thompson 1982; Reid et al., 2014)

2.2. Geological Settings of the study area

Geomorphological, the northern part of the Western Desert in Egypt is the low part in elevation compared to the rest of Western Sahara, the slope towards the north and contains the Qattara depression, which represents the lowest area 145 meters below sea level, as well as the limestone plateau (Marmarica plateau). It is also distinguished by the presence of oases and dunes.

The stratigraphic column of the study area (Figure 2) includes most stratigraphic succession from Paleozoic to recent. The surface geological structure and outcrops of stratigraphic facies are clearly shown in (Figure 3). The paleozoic sequence is made up primarily of classics and composed of seven rock units from the base to the top Shifa, Kohla, Basur, Zieton, Desouky, Dahiffan, and Safi (Keeley, 1989). The Jurassic sequence is made up of five Formations from the base to the top, Bahrien Formation, a 549 m thickness of siltstone and sandstone, Wadi El-Natrun Formation (marine carbonate shale), Khatattba Formation, a 1201 m thickness of sandstone and shale, Masajid Formation a 450 m – 840 m thickness of dolomitic limestone, marl and shale, Sidi Barrani Formation maximum thickness is 2404 m of dolomitic limestone and shale (Norton, 1967; Hantar, 1990). The Cretaceous sequence divided into two parts; the lower one is made up of classics of the Burg Alarab Formation which consisting of 4 members Alam Elbuib Member (Matruh shale Member), Alamein dolomite Member, Dahab shale Member, Kharita clastic Member, the upper sequence considered the begging of sea transgression. It consists of three Formations, from the base to the top, Baharyia Formation, a 50 m – 501 m thickness of persistent limestone, Abu Rawash Formation consist of 7 members, A, B, C, D, E, F, G, and Khoman Formation made up of chalky limestone (Hantar, 1990). The Cenozoic sequence is made up of carbonate facies, Apollonia Formation a 250 m thickness of grey nummulitic limestone, Dabaa Formation a 230 m thickness of limestone and calcareous shale with minor siltstone (Al Far, 1966), Mamura Formation a 114 m – 401 m thickness of limestone and calcareous shale (El Akkad and Issawi, 1963), Marmarica Formation consist of limestone, dolomite, and shale.

Tectonically, the present study is considered a part of the unstable shelf of the tectonic framework of the Egyptian province. It is affected by two main phases of deformation. The first one is the Tethyan rifting phase, which formed rift basins with NE - SW to ENE - WSW (Alamein-Razzak, Matruh, and Shoshan Basins). The extension to the south decreases and thus creates normal faults and has a slight slip (Bosworth et al., 2015; Moustafa et al., 2002). The second is Cretaceous rifting, which creates the Abu Gharadig basin.

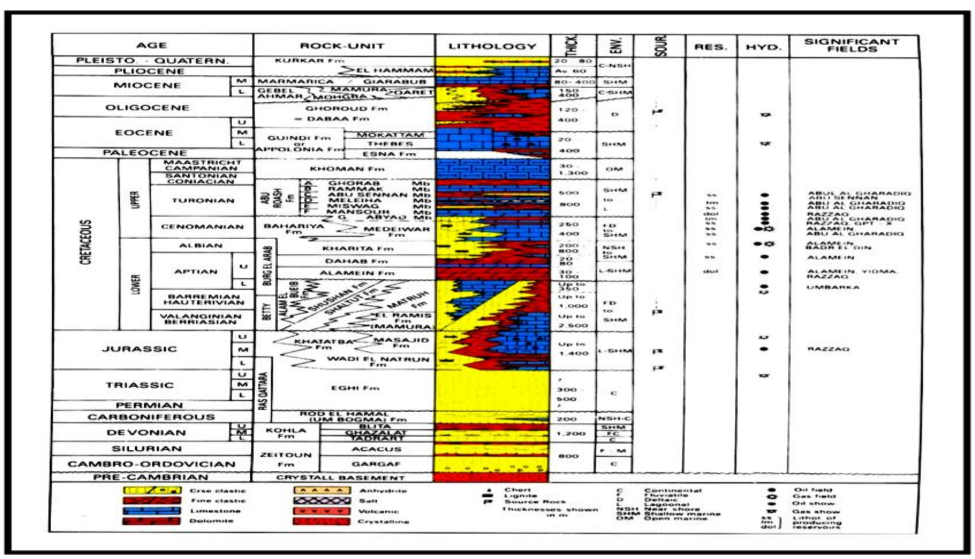

Figure 2. Subsurface stratigraphic column of the northern part of the Western Desert (Schlumberger, 1984).

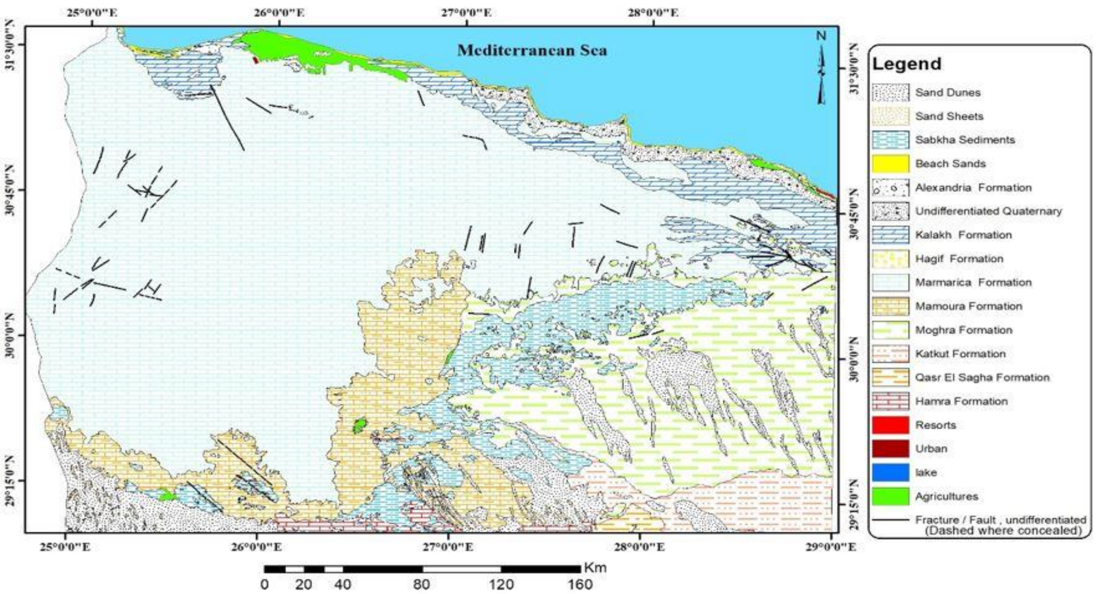

Figure 3. Geologic map of the study area (After EGPC and Conoco, 1987).

3. Results and discussion

3.1. International geodetic reference formula (IGRF) technique

The magnetic anomaly shape depends not only on its form and susceptibility to the source body but also on its magnetic orientation and direction to the regional magnetic field.

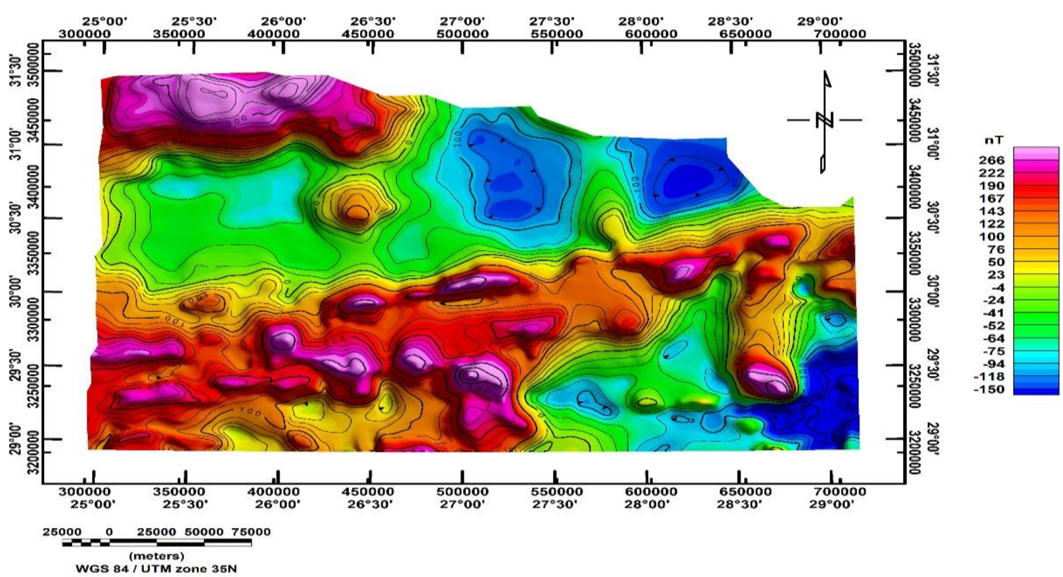

Figure 4. International Geodetic Reference Formula (IGRF) magnetic map of the study area.

The IGRF technique is used to remove the regional effects of the magnetic field by subtracting from each reading the value computed from the IGRF model. It reflects the shift of magnetic anomalies to the north due to the difference in inclination and declination of the magnetic field in the study area. The magnetic anomalies in the study area show a variation in values between -

146 nT to +600 nT (Figure 4). The highest value the magnetic anomaly has reached is +600 nT in the southern part of the study area. Northwestern and southwestern parts have a high magnetic anomaly value of more than + 300 nT. There is a significant anomaly in the southeastern part of the Abu Gharadig basin up to +500 nT; these positive values because of the high magnetic susceptibility of the rocks in these parts. These anomalies are sharp because the basement is shallow; these parts, which have positive values, represent uplifted parts in the study area. The anomalies at the northern and southeastern parts are harmful because of the low magnetic susceptibility of the rocks in these parts; these anomalies are gentle and flat because the basement is deep, and it represents Shoshan and Matruh basins in the northern part and Abu Gharadig basin in the southeastern part, which have subsidence (Haby et al., 2016). Magnetic anomalies mostly have an elliptical, elongated shape, and some anomalies are twisted. The other anomalies in the area reflect a horizontal heterogeneity of magnetic properties. The main trends in which the magnetic anomaly pattern arises E-W and NE-SW.

3.2. Butterworth filtering utilization

By using Geosoft oasis montaj version 8.4 (2015), Butterworth low pass and high pass filters applied on IGRF aeromagnetic data in the frequency domain with parameters of, degree of filter function is 8, the central wave numbers are 0.043 and 0.48 (cycle/ground unit), respectively and 0/1 A flag.

3.2.1. Butterworth low pass map

Butterworth low pass filter applied on IGRF map by Geosoft Oasis Montaj software version 8.4 (2015) with parameters of, degree of filter function is 8, the central wave number is 0.043 (cycle/ground unit), to remove the influences of the local magnetic field and its noise (Figure 5). The positive anomalies are due to high magnetic susceptibility have an elongated shape. Moreover, it takes an E-W direction with high magnitude at the northwestern and southwestern parts and a circular shape at the southeastern part, which has a short wavelength and higher frequencies, which means the causative bodies buried at shallow depths represent the uplifted parts of the study area. The intrusive body may cause it with a considerable extension. The negative anomalies are due to the low magnetic susceptibility have circular and oval shapes at the northern and southeastern parts, which have a long wavelength and lower frequencies which mean the causative bodies buried at deep depths represents subsidence parts or basins of the study area, and it has a thick sedimentary cover.

The Low Pass filter gave an impression of the uplifted parts and subsidence parts at the study area. Consequently, more potentiality for hydrocarbon and under groundwater at basins in the study area, as confirmed by the data of drilled wells, reached the basement surface in the study area (Table 1).

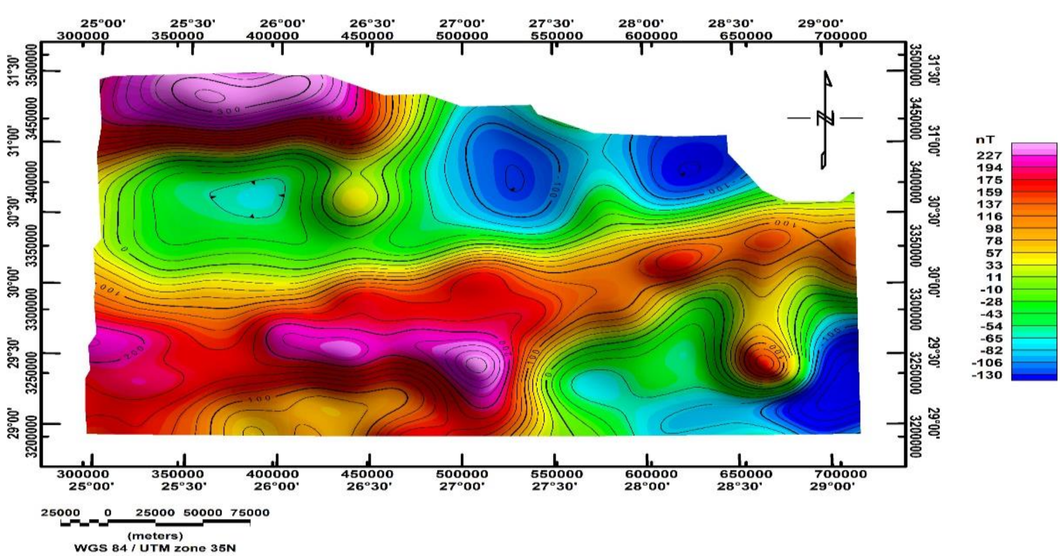

Figure 5. Butterworth low-pass filtered magnetic map (Frequency cutoff = 0.043 cycle/km and 8.0 degree).

3.2.2. Butterworth high pass map

Butterworth high pass filter applied on IGRF map by Geosoft Oasis Montaj software version 8.4 (2015) with parameters of, degree of filter function is 8, the central wave number is 0.48 (cycle/ground unit), to enhance the signal characteristics of available data. The Butterworth high pass filter is used to bring details to the map to increase noise.

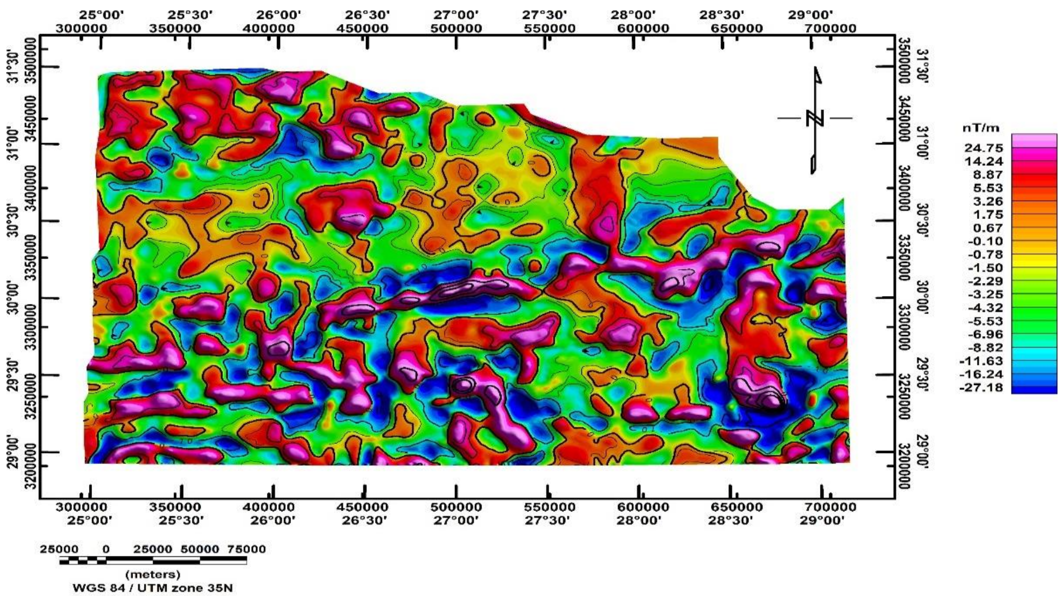

Figure 6. Butterworth high-pass filtered magnetic map (Frequency cutoff = 0.48 cycle/km and 8.0 degree).

The high pass magnetic component (Figure 6) characterized residual magnetic component clearly shows positive and negative magnetic anomalies, which have more details than those on the IGRF map. The shape of these anomalies is elongated at the southwestern and middle parts and circular shape at the southeastern part, which have short wavelength and higher frequencies. The anomalies are characterized by local variation. It happened due to the difference in their magnetic susceptibility, composition, and depths of their sources. The main trends in which the magnetic anomaly pattern arises N-S, E-W, and NE-SW.

It is clear from this method that when the profound influences of basement rocks and structure are removed, still there are influences of shallow basement rocks because these parts have been uplifted, and the structure of these parts may be extended to the surface with the same trends which clearly shown in the surface geological map (Figure 3).

3.3. Basement depth estimation

3.3.1. Radial average power spectrum technique

The technique of radial average power spectrum is utilized for basement depth estimation. It has been discussed by many authors, such as (Bhattacharyya, 1965; Spector and Grant, 1970; Garcia and Ness, 1994; Maurizio et al., 1998). The radial average power spectrum technique depends on data analysis using Fast Fourier Transform (FFT) applied on IGRF magnetic data, which calculates the depth from the spectrum. The slopes of the linear portions of the spectrum correspond to separate depth groups and provide the parameters used to design many of the enormous filters. The power spectrum of magnetic grids for depth estimation calculated by the formula:

$$H \text{ (depth)} = - \text{slope}/ 4\pi$$

The radially averaged power spectrum was calculated from IGRF magnetic data (Figure 7). Depth calculations conducted on these segments clearly show the average depth values are 6960 m and 1540 m for deep and shallow magnetic sources, respectively, when the calculated depths correlated with the drilled wells in the study area (Table 1) show a good correlation.

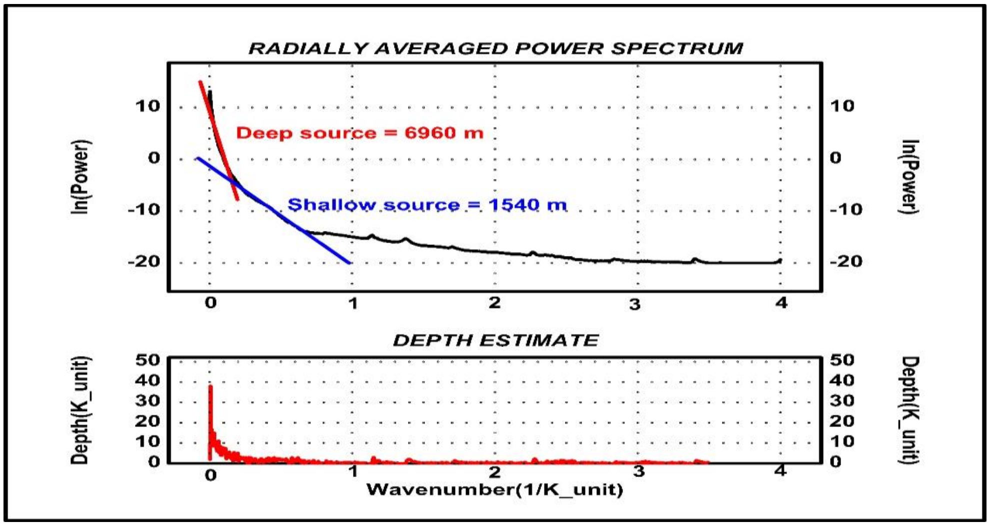

Figure 7. Radially averaged power spectrum of the IGRF magnetic data of the study area.

3.3.2. Source parameter imaging (SPI) technique

The source parameter image is utilized on the IGRF magnetic data by using Geosoft software to map the depth of magnetic sources. The SPI is a technique that depends on the extension of complex Analytical signals to estimate magnetic depths (Phillips, 2000).

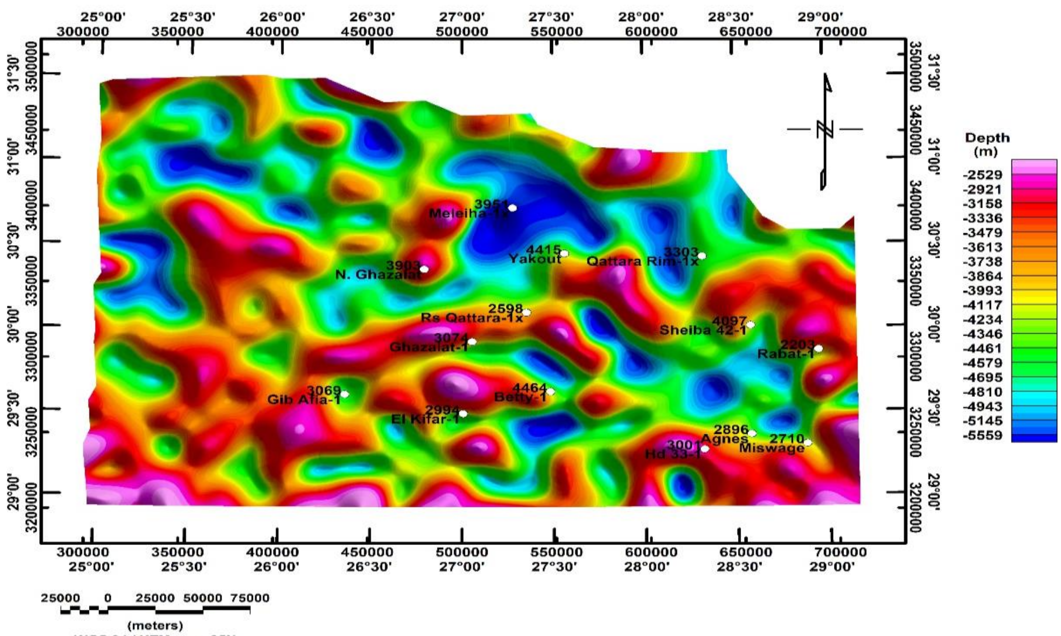

Figure 8. Basement depth from source parameter imaging (SPI) technique with the plot of drilled boreholes

The SPI solutions show the contact locations and depth of basement rocks. Based on the SPI map, the depth of magnetic sources ranges from 2529 m to 5559 m. As indicated from the SPI method (Figure 8), the violent to red colors are represented shallow depths between 2529 to 3500 m, where the orange to yellow represents intermediate depths between 3500 to 4150 m, while the green represents high depths between 4150 to 4700m. Finally, the pale blue and blue colors represent depths between 4700 to 5559 m and above. The basement rock depth values calculated by this method are very similar to the depths of drilled wells in the study area, and the difference in the depth values calculated by the Source Parameter Imaging technique may be due to the difference in the magnetic properties of the subsurface rocks in the location of boreholes (Table 1).

Areas with a higher depth to the basement are thicker in the sedimentary cover. The northern portion and southeastern parts of the study area are thicker than the southern portion of the sedimentary cover, these parts represent the main sedimentary basins (Shoshan basin, Matruh basin, and Abu Gharadig basin) which verified by drilled wells, so these parts are a good site for under groundwater and hydrocarbon exploration.

Table 1. The drilling wells reached basement rocks and estimated depth with SPI and ED techniques in the study area. The depth of drilled boreholes was used as the known point at each well for adjusting and calibrating the magnetic data process. The locations of these wells are shown in (Figure 8).

Well Name	**SPI Depth (m)**	**ED Depth (m)**	**Drilled bore holes Depth**(m)
Gib Afia-1	4320	2832	3069
N. Ghazalat	2754	3752	3903
El Kifar-1	3854	3000	2994
Rs Qattara-1x	3325	2721	2598
Ghazalat-1	2768	2865	3074
Betty-1	4065	3061	4464
Rabat-1	2906	2453	2203
Qattara Rim-1x	4062	3190	3303
Agnes	3981	3280	2896
Miswage	3900	3895	2710
Hd 33-1	3029	2797	3000.7
Yakout	4036	2831	4414.9
Sheiba 42-1	3543	3609	4097
Meleiha-1x	3387	2850	3951.39

3.3.3. 3-D Euler deconvolution technique

Euler deconvolution technique was applied on the IGRF magnetic map of the investigated area using Geosoft oasis montaj version 8.4 (2015). The Euler solutions are calculated by applying structure index (SI) equal to zero to detect magnetic contacts (Durrheim and Cooper, 1998; Reid et al., 1990; Thompson, 1982). Euler deconvolution with the value of one structure index is to detect thin sheets edges (sill and dike), with the value of two is to detect line sources (pipelines and kimberlitic pipes) and with the value of three is to detect sphere or compact body at a distance.

The following represents a brief description of the obtained Euler map with the value of zero structure index, which is used mainly to detect the geological contacts between central lithological units with different magnetic susceptibilities. The inspection of the obtained classified Euler map with the value of zero structure index (Figure 9) shows that the obtained Euler anomalies range from 1065 to 4526 meters in depth. The maximum value is observed at scattered parts. Also, it is noted that the depth increases northward the study area. Most external contacts extend in the NE-SW direction; these lineaments increased in the southeast and the west directions. So, most of these lineaments coincide with the surface lineament distribution traced from the geological map of the study area (Figure 3). The close inspection of Euler anomaly clusters indicates that the most profound trends are in the northern and southeastern parts of the area under investigation extending in the N-S and NE-SW directions. These parts of maximum depth may represent subsided blocks of the basement.

On the other hand, the Euler anomaly trends having shallower depth values are observed in the northwestern, southwestern, and central parts. The location of these shallow Euler trends delimits the possible boundaries of the uplifted basement blocks found in the study area. Using structural index zero gives depth values more similar to those estimated by different depth estimation procedures that may be due to the magnetic contacts usually appear on surfaces of magnetic contrast, which is related to lithology (Hantar, 1990). When the calculated depth values are compared with the depth values of the drilled Wells, it was very similar, and the difference in the depth values calculated by Euler Deconvolution technique may be due to the difference in the magnetic properties of the subsurface rocks in the location of boreholes (Table 1). The IGRF map was used as a background to show the complete coincidence between the calculated plotted contacts and the boundaries of the magnetic anomalies.

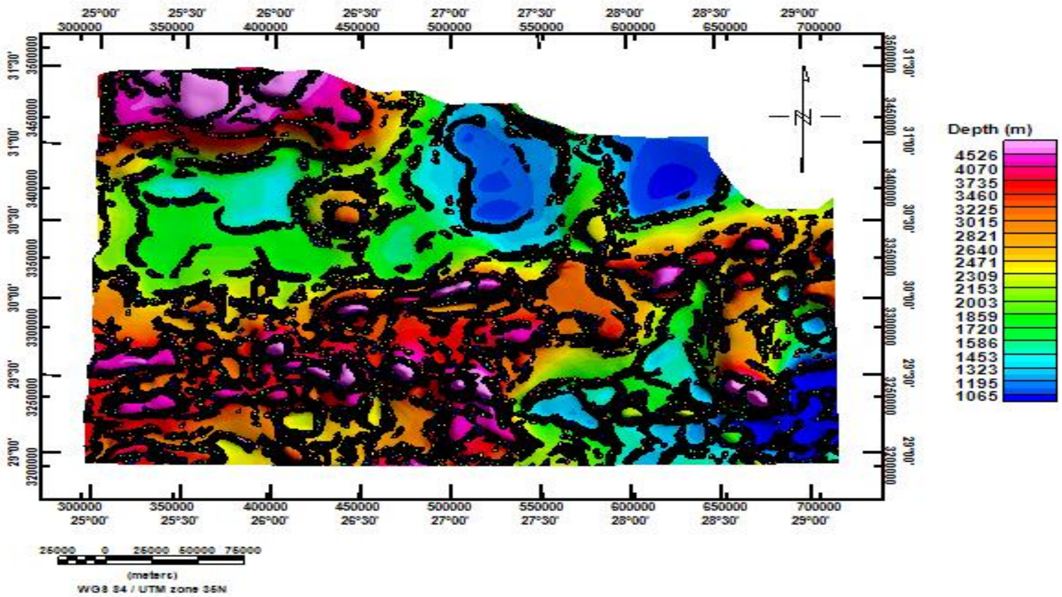

Figure 9. IGRF shaded relief map taking as a background to the Euler map (with structural index equal to zero for the study area).

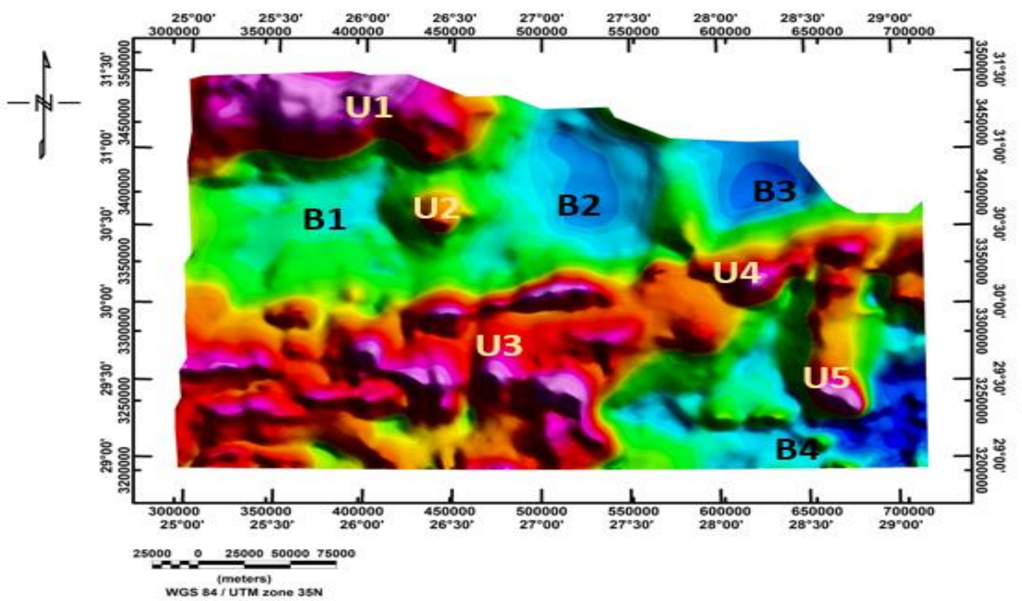

Figure 10. IGRF map shows the location of main basins and uplifts in the study area. Basins, B1 Shoshan, B2 Matruh, B3 Alamien, B4 Abu Gharadig. Uplifts, U1 Dawadi El Ramis, U2 Siqifa, U3 Gibb Afia Ghazalat, U4 Dabaa, U5 Qattara.

4. Conclusion

The present study focuses on determining basement depth in the northwestern part of Egypt by interpreting aeromagnetic data. The northern part of the western desert represents Egypt's essential oil production and gas provenances, and agricultural projects. The Butterworth High pass technique was applied on the IGRF map to improve the signals of local anomalies. The Butterworth low pass filter technique was applied on the IGRF map to remove local magnetic field influences and noise. The depth to basement estimated by the radial average power spectrum of IGRF map in addition to source imaging (SPI) technique in which results controlled by data of drilled wells in the study area, the basement depth in the area under investigation ranges between 2.5 km and 5.5 km in the study area, which has a good match with the drilled boreholes at the study area. The basement depth increases northward of the study area; the northern part represents a thick sedimentary cover, which tends to be a promising hydrocarbon and groundwater exploration area. Results *denote* that northern and southeastern parts distinguish deeper basement sources; the depth reaches 5559 m. These parts have a thick sedimentary cover due to the subsidence of these parts, which represent the basins that have the potentiality for hydrocarbon and underground water exploration. These basins are Shoshan, Matruh, Alamein, and Abu Gharadig, basins respectively, while the northwestern, southwestern, and central parts distinguish shallower basement sources, the depth reaches 1540 m, and these parts have a thin sedimentary cover due to uplift of these parts, which have less potentiality for hydrocarbon or underground water exploration.

Conflicts of interest. There are no conflicts of interest.

ORCID
Gamal Zidan Abdelaal: https://orcid.org/0000-0001-8441-9789
Mohamed Kamel Mohamed Mousa: https://orcid.org/0000-0002-9951-1905
Mohamed Osman Ebraheem: https://orcid.org/0000-0002-4417-4243

References

Abdine, A.S. (1974). Oil and gas discoveries in the Northern Western Desert of Egypt. In: 4th Exploration Seminar. E.G.P.C., Cairo, Egypt, pp.1-27.

Abu El-Ata, A.S., Ahmed, A.El-K., Shraf, E.G., Sami, H.A.A. & Marwan, A.Al.-B. (2013). Applications of aeromagnetic data to detect the Basement Tectonics of Eastern Yemen region, Egyptian Journal of Petroleum, 22, 277-292.

Adel, K., Mohamed, H.H.G. & Lamees, M. (2016). Integration between well logging and seismic reflection techniques for structural analysis and reservoir characterizations, Abu El Gharadig basin, Egypt, NRIAG Journal of Astronomy and Geophysics, 5(2), 362-379.

Al Far, D.M. (1966). Geology and coal deposits of Gebel Maghara, north Sinai, Egypt. Geological Survey of Egypt, 37, 59.

Ball J. (1927). Problems of the Libyan Desert. Geog Jour LXX:21–38,105–128 and 209–224 .

Bayoumi, A. (1996). The influence of interaction of depositional environment and syn sedimentary tectonics on the development of some Late Cretaceous source rocks, Abu Gharadig Basin, Western Desert, Egypt. EGPC 2, 475-496.

Bayoumi, A.I. & Lotfy, H.I. (1989). Modes of structural evolution of Abu Gharadig Basin, Western desert of Egypt as deduced from seismic data. Journal of African Earth Sciences, 9(2), 273-287.

Bhattacharyya, B. (1978). Computer modeling in gravity and magnetic interpretation. Geophysics, 43, 912-929.

Bhattacharyya, B.K. (1965). Two-dimensional harmonic analysis as a tool for magnetic interpretation. Geophysics, 30, 829-857.

Bosworth, W., Drummond, M., Abrams, M. & Thompson, M. (2015a). Jurassic rift initiation source rock in the Western Desert, Egypt— relevance to exploration in other continental rift systems. In: Petroleum systems in rift basins, pp615–650.

Cassano, E. & Rocca, F. (1975). Interpretation of magnetic anomalies using spectral estimation techniques. Geophysical Prospecting, 23, 663-681.

CONOCO (1987). Geological map of Egypt (scale 1: 500,000), compiled by the EGPC and CONOCO Coral, Cairo, Egypt.

Donaldson, W.S., Plint, A.G. & Longstaffe, F.J. (1998). Basement tectonic control on distribution of the shallow marine Bad Heart Formation, Peace River arch area, northwest Alberta. Bulletin of Canadian Petroleum Geology 46, 476-495.

Durrheim, R.J. & Cooper, G.R.J. (1998). EULDEP: a program for the Euler deconvolution of magnetic and gravity data. Computers & Geosciences, 24, 545-550.

El Akkad, S. and Issawi, B. (1963). Geology and iron ore deposits of Bahariya Oasis. Geological Survey of Egypt, 18, 300.

El Saadany, M. & Mahmoud, A. (2008). Sequential structural restoration of the BED1 field area, Abu Gharadig basin, Western Desert, Egypt. MERC Ain Shams Univ Earth Sci Ser 22, 25-46.

Elkhodary, S.T. & Youssef, M.A.S. (2013). Integrated potential field study on the subsurface structural characterization of the area North Bahariya Oasis, Western Desert, Egypt. Arab Journal of Geoscience, 6, 3185-3200.

Fedi, M., Quarta, T. & De Santis, A. (1997). Inherent Power-Law behavior of magnetic field power spectra from Spector and Grant ensemble. Geophysics, 62,1150-1143.

Garcia, J.G., Ness, G.E., (1994). Inversion of the power spectrum from magnetic anomalies. Geophysics 59 (3), 391–401.

Geosoft Program (Oasis Montaj), Version 8.4, (2015). Geosoft Mapping and Application System, Inc.

Gerard, A. & Debeglia, N. (1975). Automatic three-dimensional modeling for the interpretation of gravity or magnetic anomalies. Geophysics, 40(6), 1014-1034.

Haby S.M., Senosy M.M. & Abd el Zaher, M. (2016). Interactive interpretation of airborne gravity, magnetic, and drill-hole data within the crustal framework of the northern Western Desert, Egypt. Journal of Applied Geophysics, 134, 291-302.

Hahn, A., Kind, E.G. & Mishara, D.C. (1976). Depth estimation of magnetic sources by means of Fourier amplitude spectra. Geophysical Prospecting, 24, 287-308.

Hamza, H. & Graba, I. (2010). Challenges of exploration and utilization of hydrocarbons in the Sokoto Basin. Paper presented at International Conference on the Potentials of Prospecting for Hydrocarbons in the Sokoto Basin, Usmanu Danfodio University Sokoto, Nigeria.

Hantar, G. (1990). North western desert. In: Said, R. (Ed.). The Geology of Egypt. A.A. Balkema, Rotterdam, Brookfield, pp. 293.

Hesham S.Z. & Hesham T. (2016). Application of high-pass filtering techniques on gravity and magnetic data of the eastern Qattara Depression area, Western Desert, Egypt, NRIAG Journal of Astronomy and Geophysics, 5, 106-123.

Ibraheem, I.M., Elawadi, E.A. & El-Qady, G.M. (2018). Structural interpretation of aeromagnetic data for the Wadi El Natrun area, northwestern desert, Egypt. Journal of African Earth Sciences, 139, 14-25.

Keeley, M.L. (1989). The Paleozoic history of the Western Desert of Egypt. Basin Research, 2, 35-48.

Khalil, A., Tharwat H.A., Hassan S.S. & Waheed H.M. (2016). Inferring the subsurface basement depth and the structural trends as deduced from aeromagnetic data at West Beni Suef area, Western Desert, Egypt, NRIAG. Journal of Astronomy and Geophysics, 5, 380-392.

Kivior, I. & Boyd, D. (1998). Interpretation of the aeromagnetic experimental survey in the Eromanga/Cooper basin. Canadian Journal of Exploration Geophysics, 34, 58e66.

Kumar D., Murthy N.S.K., Nayak G.K. & Ahmed S. (2006). Utility of magnetic data in delineation of groundwater potential zones in hard rock terrain. Current Science, 91, 1456-1458.

Maurizio, F., Tatina, Q. & Angelo, S. (1998). Exploration of a lignite bearing in Northern Ireland, using ground magnetic. Geophysics, 62(4), 1143-1150.

Metwaly, M., El-Qady, G., Massoud, U., El-Kenawy, A., Matsushima, J. & Al-Arifi, N. (2009). Integrated geoelectrical survey for groundwater and shallow subsurface evaluation: case study at Siliyin spring, El-Fayoum Egypt. International Journal of Earth Sciences, 99, 1427-1436.

Moustafa, AR. (2002). Structural style and timing of Syrian arc deformation in northern Egypt. AAPG International meeting, Cairo, Oct 2002.

El Redini, N.A.H., Bakr, A.M.A. & Dahroug, S.M. (2017). Seismic data interpretation for hydrocarbon potential, for Safwa/Sabbar field, East Ghazalat onshore area, Abu Gharadig basin, Western Desert, Egypt. NRIAG Journal of Astronomy and Geophysics, http://dx.doi.org/10.1016/j.nrjag.2017.01.003.

Nessim, M., Abedi, M.H. & El Toukhy, M. (1992). 3D Seismic: An exploration & production tool for the Abu Gharadig Basin, Egypt. Conference Paper published in 54th EAEG Meeting.

Norton, P. (1967). Rock-stratigraphic nomenclatures of the Western Desert, Egypt. Egypt Petrol. Corp.

Phillips, J. D. (2000). locating magnetic contacts: a comparison of the horizontal gradient, analytical signal, and local wavenumber methods. society of exploration Geophysicists, Abstracts with programs, Calgary, 2000.

Rabeh, T., Bedair, S. & Abd El Zaher, M. (2017). Integration of geophysical tools for delineating structures controlling the groundwater reservoirs at Baharia Oasis, Western Dessert, Egypt. Journal of Geosciences, http://dx.doi.org/10.1007/s12303-016-0072-3.

Reid, A.B., Allsop, J.M., Granser, H., Millett, A.J. & Somerton, I.W. (1990). Magnetic interpretation in three dimensions using Euler Deconvolution. Geophysics, 55, 80-90.

Reid, A.B., Ebbing, J.O. & Susan, S.J. (2014). Avoidable Euler Errors—The use and abuse of Euler Deconvolution applied to potential fields. Geophysical Prospecting, 62, 1162-1168.

Reynolds, J. (1997). An introduction to applied and environmental geophysics, John Wiley & sons, Chester, 2nd edition, 710p.

Ross, M.G. & Eaton, D.W. (1999). Basement reactivation in the Alberta Basin; observation constraints and mechanical rationale. Bulletin of Canadian Petroleum Geology, 47(4), 391-411.

Saibi, H., Aboud, E. & Gottsmann, J. (2015). Curie point depth from spectral analysis of aero- magnetic data for geothermal reconnaissance in Afghanistan. Journal of African Earth Sciences, 9111, 92.

Schlumberger (1984). EGPC Western desert, Oil and Gasfieldas, 1992; and Shaarkawy, GUPCO in M. Abdel Halim, EGPC 1994, Stratigraphic column of the North western desert.

Shahin, A.N. (1989). Undiscovered Reserves in the Northern Western Desert, Egypt: Application of Quantitative Modelling to Petroleum Exploration Proc. vol. 3. 28th Int. Geol. Cong, Washington, D.C, pp.3-82.

Spector, A. & Grant, F.S. (1970). Statistical models for interpreting aeromagnetic data Geophysics 35, 293–302.

Subrahmanyam, M. & Gebissa, F.T. (2017). Performance evaluation of spectral analysis and Werner deconvolution interpretation techniques in magnetic method. Journal of Applied Geophysics, 138, 102e113.

Thompson, D.T. (1973). Identification of Magnetic Source Types Using Equivalent Simple Models. Fall Annual AGU Meeting, San Francisco, 10-13 December 1973.

Thompson, D.T. (1982). EULDPH: A New Technique for Making Computer Assisted Depth Estimates from Magnetic Data. Geophysics, 47, 31-37.

Thurston, J.B. & Smith, R.S. (1997). Automatic conversion of magnetic data to depth, dip and susceptibility contrast using the SPITM method. Geophysics, 62, 807-813.

Yousif, M., van Gelder, R. & Bubenzer, O. (2016). Hydrogeological investigation of shallow aquifers in an arid data-scarce coastal region (El Daba´a, northwestern Egypt). Hydrogeology Journal, 24, 159-179.